

RESEARCH

Open Access



# Metabolic engineering of *Corynebacterium crenatum* for enhanced L-tyrosine production from mannitol and glucose

Gang Yang<sup>1</sup>, Sicheng Xiong<sup>1</sup>, Mingzhu Huang<sup>1</sup>, Bin Liu<sup>1</sup>, Yanna Shao<sup>2</sup> and Xuelan Chen<sup>1,2\*</sup>

## Abstract

**Background** L-Tyrosine (L-Tyr) is a significant aromatic amino acid that is experiencing an increasing demand in the market due to its distinctive characteristics. Traditional production methods exhibit various limitations, prompting researchers to place greater emphasis on microbial synthesis as an alternative approach.

**Results** Here, we developed a metabolic engineering-based method for efficient production of L-Tyr from *Corynebacterium crenatum*, including the elimination of competing pathways, the overexpression of *aroB*, *aroD*, and *aroE*, and the introduction of the mutated *E. coli tyrA<sup>fbt</sup>* gene for elevating L-Tyr generation. Moreover, the *mtlR* gene was knocked out, and the *mtlD* and *pfkB* genes were overexpressed, allowing *C. crenatum* to produce L-Tyr from mannitol. The L-Tyr production achieved 6.42 g/L at a glucose-to-mannitol ratio of 3:1 in a shake flask, which was 16.9% higher than that of glucose alone. Notably, the L-Tyr production of the fed-batch fermentation was elevated to 34.6 g/L, exhibiting the highest titers among those of *C. glutamicum* previously reported.

**Conclusion** The importance of this research is underscored by its pioneering application of mannitol as a carbon source for the biosynthesis of L-Tyr, as well as its examination of the influence of mannitol-associated genes in microbial metabolism. A promising platform is provided for the production of target compounds that does not compete with human food source.

**Keywords** *Corynebacterium crenatum*, Mannitol, L-tyrosine, Mixed carbon source

## Background

Aromatic amino acids hold significant value across diverse industries such as the food, cosmetic, and pharmaceutical industries owing to their unique structural properties [1–3]. However, the incomprehensive understanding of its functions in human health cause the industrial production of L-tyrosine (L-Tyr) to receive

limited research attention. In recent years, the market demand for L-Tyr has grown because of the discovery that it plays a pivotal role in enhancing nervous system development, treating depression, and functioning as an antioxidant [4–6]. Furthermore, L-Tyr acts as a crucial precursor in the synthesis of high-quality aromatic compounds like resveratrol and p-coumaric acid [7, 8].

Conventional methods of L-Tyr synthesis primarily encompass two techniques: chemical synthesis and enzymatic hydrolysis [9]. The entire process of chemical synthesis necessitates stringent conditions and the use of various chemical reagents that may potentially result in environmental pollution [10]. Meanwhile, enzymatic

\*Correspondence:

Xuelan Chen  
xuelanchen162@163.com

<sup>1</sup>School of Life Sciences, School of Health, Jiangxi Normal University, Nanchang 330022, China

<sup>2</sup>School of Health, Jiangxi Normal University, Nanchang 330022, China



© The Author(s) 2024. **Open Access** This article is licensed under a Creative Commons Attribution-NonCommercial-NoDerivatives 4.0 International License, which permits any non-commercial use, sharing, distribution and reproduction in any medium or format, as long as you give appropriate credit to the original author(s) and the source, provide a link to the Creative Commons licence, and indicate if you modified the licensed material. You do not have permission under this licence to share adapted material derived from this article or parts of it. The images or other third party material in this article are included in the article's Creative Commons licence, unless indicated otherwise in a credit line to the material. If material is not included in the article's Creative Commons licence and your intended use is not permitted by statutory regulation or exceeds the permitted use, you will need to obtain permission directly from the copyright holder. To view a copy of this licence, visit <http://creativecommons.org/licenses/by-nc-nd/4.0/>.

approaches make use of specific enzymes to structurally alter particular substrates to L-Tyr [11]. Nevertheless, this method is costly and lacks stability. Therefore, attaining a green, cost effective, efficient, and stable way to produce L-Tyr has become a major challenge. With the progression of genetic engineering in the realm of synthetic biology, the application of metabolic engineering for synthesizing target products is garnering increased popularity among researchers [12]. Compared with the traditional methods of L-Tyr synthesis, metabolic engineering presents the advantages of eco-friendliness, efficiency, and a broad range of raw material sources [13]. By engineering microorganisms for L-Tyr synthesis, metabolic engineering offers a promising solution to the existing challenges in L-Tyr production.

Currently, the microorganisms predominantly utilized for synthesizing L-Tyr encompass *Escherichia coli* [14], *Corynebacterium glutamicum* [15], and *Saccharomyces cerevisiae* [16]. Among them, researchers have previously achieved a shake-flask fermentation titer of 6.3 g/L by modifying the production pathway for L-Tyr [17]. *C. crenatum*, a Gram-positive bacterium isolated from soil by Chinese scholars in 1965, is a subspecies of *C. glutamicum* [18]. In contrast to *E. coli*, *C. crenatum* is extensively used in the synthesis of various chemicals due to

its superior genetic manipulability, safety, and low pathogenicity as well as *C. glutamicum* [19]. Consequently, *C. crenatum* is widely utilized to produce amino acids [20], chemicals [21], and natural products [22]. *C. crenatum* also possesses complete L-Tyr synthesis pathway in vivo, making it a well-established host for L-Tyr production.

As the global population continues to expand, the issue of food scarcity has become a common challenge faced by humanity [23]. It has become a key direction for researchers to avoid using carbon sources that compete with human food sources during industrial production. Mannitol, a six-carbon polyol extracted from brown algal cells, has emerged as a promising third-generation carbon source for synthesizing various substances [24]. For example, *C. glutamicum* was successfully modified by knocking out the *mtlR* gene, enabling it to utilize mannitol and produce L-ornithine with a titer of 54.56 g/L [25]. Similarly, through adaptive evolution in the laboratory, *Saccharomyces cerevisiae*'s ability to utilize mannitol was enhanced, allowing it to produce valencene at a titer of 5.61 g/L [26]. These studies show that mannitol can be used to synthesize a variety of substances.

The synthesis pathway of L-Tyr is illustrated in Fig. 1. After glucose is absorbed into the body by *C. crenatum*, two important precursors, erythrose-4-phosphate

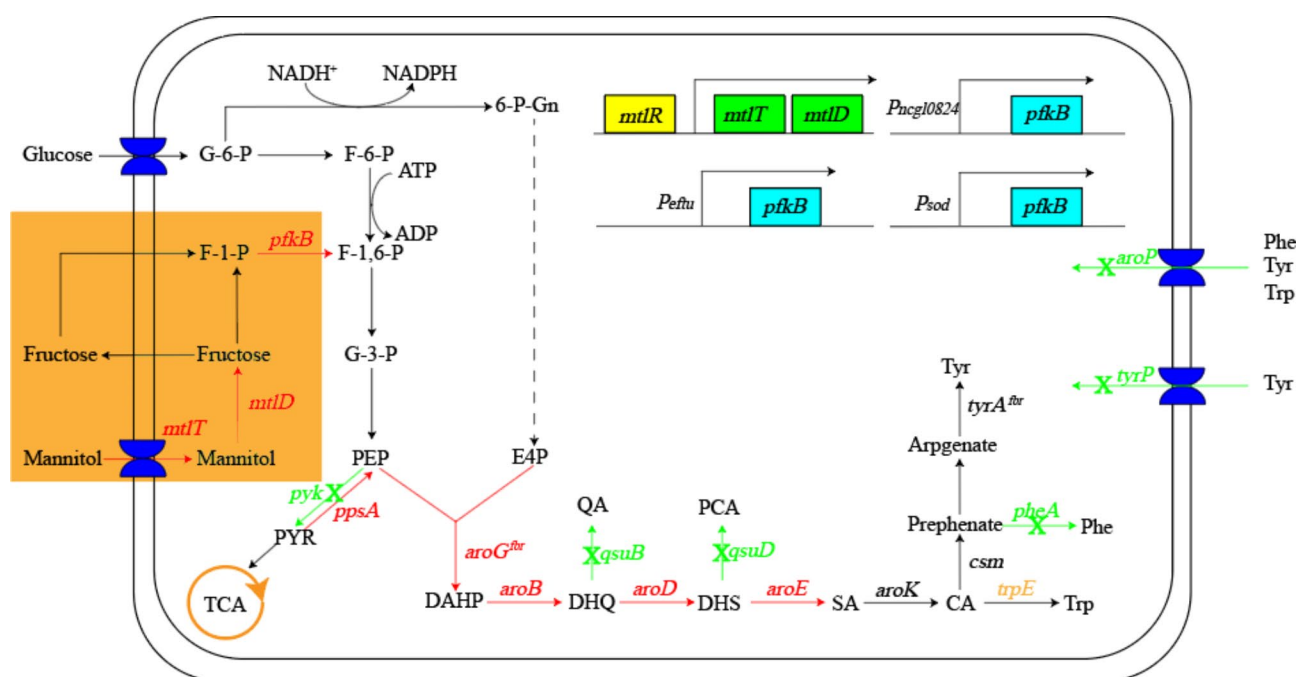


**Fig. 1** Metabolic pathway of tyrosine synthesis in *Corynebacterium crenatum*. Red font indicates that the gene is overexpressed. The green "x" indicates that the gene has been knocked out. *mtlR* encodes mannitol repressor; *mtlT* encodes mannitol transporter; *aroG* encodes 3-deoxy-7-phosphoheptulonate synthase from *E. coli*; *aroB* encodes 3-dehydroquinate synthase; *aroD* encodes putative 3-dehydroquinate dehydratase; *aroE* encodes shikimate dehydrogenase; *qsuB* encodes 3-dehydroshikimate dehydratase; *qsuD* encodes shikimate dehydrogenase; *trpE* encodes anthranilate synthase; *pheA* encodes prephenate dehydratase; *tyrA* encodes arogenate dehydrogenase from *E. coli*; *aroP* encodes aromatic amino acid transport protein; *tyrP* encodes tyrosine permease; *pyk* encodes pyruvate kinase; *ppsA* encodes phosphoenolpyruvate synthase; *mtlD* encodes mannitol dehydrogenase; *mtlR* encodes mannitol repressor; *pfkB* encodes fructose-1-phosphate kinase; DAHP: 3-deoxy-7-phosphoheptulonate; DHQ: 3-dehydroquinic acid; DHS: 3-dehydroshikimic acid; SA: shikimic acid; CA: chorismate acid

(E4P) and phosphoenolpyruvate (PEP), are produced through the pentose phosphate pathway and glycolysis, respectively. 3-Deoxy-D-arabinopyranosyl-7-phosphate (DAHP) is synthesized through the action of a synthetase that utilizes E4P and PEP. Subsequently, DAHP is converted into chorismic acid through the action of enzymes encoded by the *aroB*, *aroD*, *aroE*, and *aroK* genes. Chorismic acid serve as common precursors for three aromatic amino acids, and a portion of these chorismic acid is transformed into p-aminophenylpyruvic acid, catalyzed by the bifunctional enzyme TyrA. This compound is subsequently converted into the final product, L-Tyr, by the enzyme encoded by the *tyrB* gene.

When mannitol is utilized by *C. crenatum*, it is transported intracellularly through the transporter protein encoded by the *mtlT* gene. Subsequently, mannitol is converted into fructose by mannitol 2-dehydrogenase, which is encoded by the *mtlD* gene. Most of this fructose is then converted into fructose-1-phosphate(F-1-P). The remainder is secreted extracellularly, reabsorbed, and converted into F-1-P [27]. Finally, F-1-P is converted by the enzyme encoded by the *pfkB* gene into fructose-1,6-bisphosphate, which enters the pentose phosphate pathway.

Herein, we constructed the initial strain for L-Tyr production using mannitol by genetically modifying *C. crenatum* AS1.542. The specific genetic engineering strategy is illustrated in Fig. 1. We successfully co-cultivated glucose and mannitol to produce L-Tyr, achieving a remarkable titer of 6.42 g/L for shake-flask fermentation and

34.6 g/L for fed-batch fermentation. Notably, these surpassed the highest recorded titer of *C. glutamicum*, providing a valuable reference for the microbial utilization of mannitol and glucose in producing other chemicals.

## Materials and methods

### Genetic techniques

The strain used in this study was *C. crenatum* AS. 1.542. All primers were purchased from Nanjing Jinsirui Company. The plasmid vector used was pK18mobsacB [28]. After the target plasmid was constructed, it was introduced into *E. coli* DH5 $\alpha$  strain through heat shock transformation for plasmid amplification, and the amplified plasmid was extracted again. Cultivation of *E. coli* in a shaker at 37 °C by using LB medium. The plasmid was introduced into *C. crenatum* competent cell using the electroporation method. Preparation of *C. crenatum* competent cell by the glycerol method [29]. The receptor medium consisted of LB medium with an additional 3% glycine and 0.1% Tween 80. Through two homologous recombination steps, the pK18mobsacB plasmid was utilized to transport the kanamycin resistance site and the sucrose lethal gene for the final screening process, resulting in the acquisition of the target strain [30] Table 1.

### Flask fermentation

Before flask fermentation, the strains were cultured and activated in 10 mL of Brain Heart Infusion (BHI) medium overnight. After activation, add 1–2 mL of the bacterial solution were added to 25 mL of CGXII medium [31], followed by the addition of appropriate amounts of various carbon sources, respectively. The strains were cultured on a shaking table at 30 °C with a speed of 180 rpm/min. A certain amount of L-Phenylalanine was added to the medium if necessary.

### Fed-batch fermentation

Before fed-batch fermentation process, the strain needs an activation period of 24 h using the seed medium which contains 80 g/L of a mixed carbon source (60 g/L glucose and 20 g/L mannitol), 20 g/L (NH<sub>4</sub>)<sub>2</sub>SO<sub>4</sub>, 10 g/L yeast extract, 5 g/L urea, 0.25 g/L MgSO<sub>4</sub>, 2 g/L KH<sub>2</sub>PO<sub>4</sub>, 2 g/L K<sub>2</sub>HPO<sub>4</sub>, 5 ml/L of a trace metal solution (composed of 3.0 g/L MnSO<sub>4</sub>·5H<sub>2</sub>O, 2.5 g/L CaCl<sub>2</sub>·2H<sub>2</sub>O, 2 g/L FeSO<sub>4</sub>·7H<sub>2</sub>O, 0.2 g/L ZnSO<sub>4</sub>·7H<sub>2</sub>O, 0.05 g/L CuSO<sub>4</sub>·5H<sub>2</sub>O), and 10 g/L beef extract. After a 24-hour incubation period, inoculate the bacterial solution into a 5 L fermenter at a 10% inoculation rate. The fermentation media used for scaling up fermentation in 5 L fermenters mainly contain 40 g/L of a mixed carbon source (30 g/L glucose and 10 g/L mannitol), 20 g/L (NH<sub>4</sub>)<sub>2</sub>SO<sub>4</sub>, 10 g/L yeast extract, 5 g/L urea, 2 g/L MgSO<sub>4</sub>, 2 g/L KH<sub>2</sub>PO<sub>4</sub>, 2 g/L K<sub>2</sub>HPO<sub>4</sub>, and 5 ml/L of trace metals. The fermentation temperature is controlled at 30 °C, and the rotational

**Table 1** Strains constructed in this study

Strains	Description	Reference
<i>Corynebacterium crenatum</i> AS 1.542	mutant strain of wild-type <i>C. crenatum</i>	Lab stock This work
CCGT01	<i>aroG<sub>Ec</sub><sup>fbr</sup></i> mutant of <i>Corynebacterium crenatum</i> AS1.542	
CCGT02	<i>trpE</i> -TTG mutant of CCGT01	This work
CCGT03	$\Delta$ <i>pheA</i> mutant of CCGT02	This work
CCGT04	$\Delta$ <i>qsuB</i> , $\Delta$ <i>qsuD</i> mutant of CCGT03	This work
CCGT05	:: <i>aroB</i> , <i>aroD</i> , <i>aroE</i> mutant of CCGT04	This work
CCGT06	<i>tyrA<sub>Ec</sub><sup>fbr</sup></i> mutant of CCGT05	This work
CCGT06A	<i>tyrA<sub>Ec</sub></i> mutant of CCGT05	This work
CCGT07	:: <i>ppsA</i> mutant of CCGT06	This work
CCGT08	$\Delta$ <i>pyk</i> mutant of CCGT06	This work
CCGT09	:: <i>ppsA</i> mutant of CCGT08	This work
CCGT10	$\Delta$ <i>tyrP</i> mutant of CCGT09	This work
CCGT11	$\Delta$ <i>aroP</i> mutant of CCGT09	This work
CCGT12	$\Delta$ <i>aroP</i> mutant of CCGT10	This work
CCMT01	$\Delta$ <i>mtlR</i> mutant of CCGT10	This work
CCMT02	:: <i>mtlD</i> mutant of CCMT01	This work
CCMT03	:: <i>mtlTD</i> mutant of CCMT01	This work
CCMT04	P <sub>ncgl0824</sub> :: <i>pfkB</i> mutant of CCMT02	This work
CCMT05	P <sub>sod</sub> :: <i>pfkB</i> mutant of CCMT02	This work
CCMT06	P <sub>efflu</sub> :: <i>pfkB</i> mutant of CCMT02	This work
<i>E. coli</i> DH5 $\alpha$	Plasmid amplification strain	Lab stock

speed is maintained at 300 rpm/min. The pH of the fermentation system was maintained at 7.0–7.5 throughout the fermentation process by using 1 mol/L HCl or ammonia. Samples were collected every six hours to measure OD<sub>600</sub>, the remaining carbon source content, and L-Tyr production. The batch replenishment ingredients primarily consist of a 600 g/L mixed carbon source (450 g/L glucose and 150 g/L mannitol), 40 g/L (NH<sub>4</sub>)<sub>2</sub>SO<sub>4</sub>, and 10 g/L yeast extract.

#### Quantitative analysis of L-Tyr

The solubility of L-Tyr in water is only 0.45 g/L at room temperature; thus, it must be completely dissolved before quantifying L-Tyr. In this study, we initially mixed a 6 mol/L HCl solution with the fermentation broth in a 1:1 ratio. Subsequently, we continuously heated and stirred the mixture to ensure the complete dissolution of the L-Tyr. After the L-Tyr was fully dissolved, the bacterial broth was centrifuged at 12,000 rpm/min for 10 min using a refrigerated high-speed centrifuge. The supernatant was collected for further testing. It was then diluted to a specific ratio. L-Tyr can be analyzed qualitatively using the Folin method and quantitatively using high-performance liquid chromatography (HPLC). L-Tyr was quantified using an Agilent C18 Zorbax column (250 mm × 4.6 mm, 5 μm) with a UV detector at 280 nm. The mobile phase consisted of 0.1 mol/L sodium acetate in methanol (90:10). The flow rate was set at 1.0 mL/min. The column temperature was 30 °C. The sample volume was 10 μL [32].

#### Quantitative analysis of glucose, mannitol and pyruvate

Quantitative analysis of glucose can be performed using the DNS method. Mannitol levels are determined using a spectrophotometer method. When *C. crenatum* utilizes mannitol, it produces a certain amount of fructose, which can interfere with mannitol detection. Therefore, it is necessary to pre-treat the samples with hydrochloric acid and then detect them at 412 nm [33]. Detection of pyruvate levels using Pyruvate (PA) Content Assay Kit.

#### Data processing and analysis

All experimental data are averages and standard deviations from three independent experiments. Creating charts using Origin and Adobe Illustrator software.

## Results

#### Construction of de novo synthetic L-Tyr strain

L-Tyr is an important aromatic amino acid produced downstream of the shikimate pathway. Thus, enhancing the shikimate pathway is essential for achieving high L-Tyr production in a strain. To construct a strain of *C. crenatum* capable of producing L-Tyr, the *aroG<sup>br</sup>* gene from *E. coli* was initially inserted to replace the native *PTA* gene. The introduction of the *aroG<sup>br</sup>* gene dramatically increased the content of DAHP, an important precursor of the shikimate pathway [34]. The resulting strain was designated as CCGT01, and the titer of L-Tyr reached 50.2 mg/L (Table 2).

The production pathway of the other two aromatic amino acids, L-tryptophan (L-Trp) and L-Phenylalanine (L-Phe), poses a significant obstacle to achieve a high titer of a specific aromatic amino acid. To increase L-Tyr production, these competing pathways must be inhibited. To weaken these two competing pathways, the *trpE* gene that encodes a key enzyme in the L-Trp production pathway, was initially modified at the start codon by changing ATG to TTG, resulting in the creation of strain CCGT02. The modified CCGT02 increased L-Tyr titer to 71.3 mg/L. Next, to reduce L-Phe synthesis, the *pheA* gene, responsible for encoding a key enzyme in the conversion of prephenate into L-Phe, was knocked out. However, the constructed strain CCGT03 failed to grow due to the absence of L-Phe. To restore the normal growth of CCGT03, 0.5 mM L-Phe was added to the medium. As shown in Fig. 2A, the maximum OD<sub>600</sub> of CCGT03 reached 7.2, indicating that the strain was not growing sufficiently well. Therefore, the next step was to restore the normal growth of the strain by adjusting the various L-Phe additions. As shown in Fig. 2A, the growth of CCGT03 was greatly restricted when L-Phe was added at an amount lower than 1 mM. Normal and robust growth resumed only when the amount added exceeded 1 mM. When L-Phe was added at a level more than 1 mM, the strain also exhibited improved the utilization of glucose (Fig. 2A). However, despite high concentrations of L-Phe promoting growth to some extent, they did not increase L-Tyr production. In fact, the highest L-Tyr titer of 2.91 g/L was achieved when L-Phe was added at 1 mM (Fig. 2B).

To block the flow of carbon sources into the competitive pathway, the *qsuB* and *qsuD* genes were knocked out in the CCGT03 strain. This led to the construction of strain CCGT04 with no significant impact on the titer of L-Tyr. In *C. crenatum*, the enzymes encoded by

**Table 2** Final OD<sub>600</sub>, L-Tyr production and yield of strain CCGT01–06

Strain	OD <sub>600</sub>	L-Tyr (g/L)	mg L-Tyr/g glucose
CCGT01	19.30 ± 0.31	0.05 ± 0.001	1.25
CCGT02	17.11 ± 1.50	0.07 ± 0.001	1.75
CCGT03	14.11 ± 0.08	2.91 ± 0.005	72.75
CCGT04	13.59 ± 0.08	2.93 ± 0.022	73.25
CCGT05	13.43 ± 0.19	3.11 ± 0.044	77.75
CCGT06	13.97 ± 1.10	3.86 ± 0.061	96.5

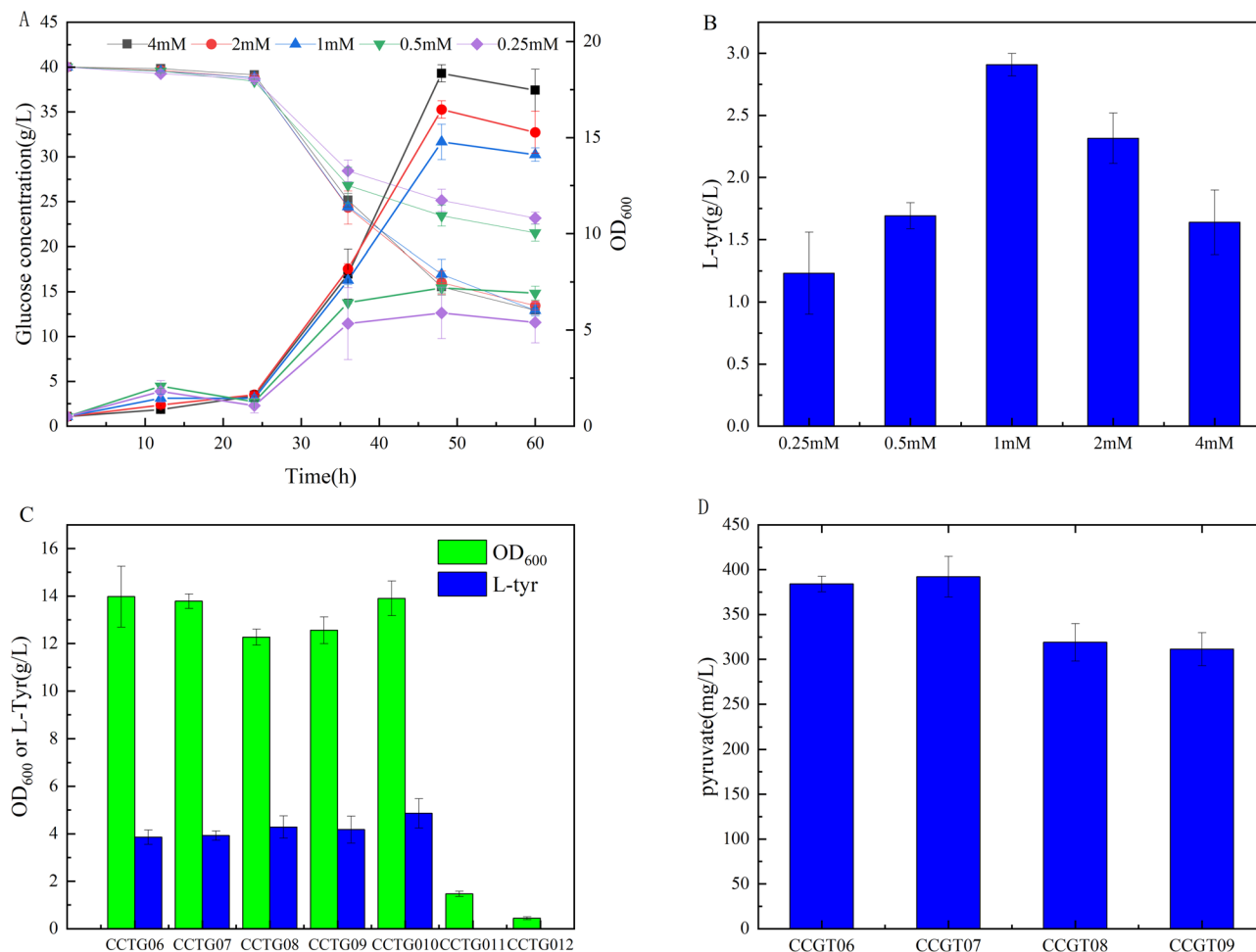


**Fig. 2** Shake-flask fermentation parameters using glucose as a carbon source. **(A)** Cell growth and glucose consumption curves of CCGT03 in different concentrations of L-Phe. **(B)** L-Tyr production of CCGT03 in different concentrations of L-Phe. **(C)** Cell growth and L-Tyr following the modification of transporter proteins and accumulation of PEP. **(D)** Pyruvate production by different strains

the *aroB*, *aroD*, and *aroE* genes facilitated the flow of carbon sources into L-Tyr. Thus, the *aroB*, *aroD*, and *aroE* genes were overexpressed using the  $P_{sod}$  to create strain CCGT05. As shown in Table 2, the L-Tyr titer of CCGT05 reached 3.11 g/L.

In *E. coli*, the *tyrA* gene encodes a bifunctional enzyme known as branched-chain amino acid transaminase/prephenate dehydratase. The L-Tyr titer was effectively increased by introducing mutations at positions 53 and 354 of *tyrA* [35]. To investigate the impact of the wild-type *tyrA* gene and the mutated *tyrA* gene from *E. coli* on the titer of L-Tyr, we constructed two strains: CCGT06 containing the mutated *tyrA* gene and CCGT06A containing the wild-type *tyrA* gene from *E. coli*. Following shake-flask fermentation, we observed no significant differences in cell growth and glucose consumption compared with those of CCGT05, as illustrated in Fig. S1A. However, the L-Tyr titer of CCGT06 reached 3.86 g/L, which was 24.1% higher than that of CCGT05. The titer of CCGT06A only increased by 8.4% to 3.37 g/L

compared with that of CCGT05. There was still a big gap between the two data (Fig. S1B). As shown in Table 2, the L-Tyr production of CCGT06 was elevated to 3.86 g/L.

To enhance the content of PEP, modifications were made to its interconversion with pyruvate. Pyruvate kinase, encoded by the *pyk* gene, facilitates the conversion of PEP into pyruvate. Meanwhile, PEP synthase, encoded by the *ppsA* gene, catalyzes the conversion of pyruvate back into PEP in *C. glutamicum* [36, 37]. In an effort to elevate the PEP content, we attempted to knock out the *pyk* gene and overexpress the *ppsA* gene (from *C. crenatum*), resulting in the data presented in Fig. 2C. The CCGT07 strain, which solely overexpressed *ppsA*, exhibited no substantial alterations in the 60th hour OD<sub>600</sub> and titer. Conversely, the CCGT08 strain, which had only the *pyk* gene knocked out, demonstrated a 10.8% enhancement in L-Tyr titer. It reached 4.28 g/L when juxtaposed with CCGT06, despite experiencing a 10.74% reduction in its 60th hour OD<sub>600</sub>. Based on the CCGT08 strain, we constructed the CCGT09 strain by overexpressing

*ppsA*. We observed that the results, in terms of  $OD_{600}$  and titer at the 60th hour, were essentially similar to those of the CCGT08 strain.

Additionally, we evaluated the pyruvate titer of the CCGT06-CCGT09 strains at hour 60. The control strain CCGT06 exhibited a pyruvate titer of 384 mg/L. Conversely, the pyruvate titer of CCGT08, which had a knockout of the *pyk* gene, was reduced by 16.9% to 319 mg/L. However, the pyruvate titer of CCGT07 and CCGT09, which overexpressed the *ppsA* gene based on CCGT06 and CCGT08, did not show significant changes compared with their respective controls (Fig. 2D).

### Modification of transporter proteins

When microbial cell factories are utilized for the efficient production of chemicals, the translocation of the target product also has a significant impact on the titer. Previous studies have shown that the *tyrP* gene encodes a tyrosine permease, which is specifically responsible for transporting L-Tyr from outside the bacterium into its interior. Conversely, the *aroP* gene encodes an aromatic amino acid transporter protein that facilitates the uptake of all three aromatic amino acids by the bacterium [38, 39]. In this study, we explored the effects of transporter proteins on cell growth and L-Tyr production through individual and cumulative knockout of *aroP* and *tyrP*. As shown in Fig. 2C, when *tyrP* was knocked out alone, namely, in strain CCGT10, L-Tyr production was augmented by 13.8% to 4.86 g/L compared with CCGT08. Surprisingly, no detriment to cell growth occurred following the knockout of *tyrP*; rather, a 13.3% increase compared with CCGT08 was found. We conjectured that the elevated concentration of L-Tyr in the fermentation broth prevented it from entering the bacteria due to the

knockout of the transporter proteins, thereby mitigating the intracellular L-Tyr damage to the cells. Following the singular knockout of *aroP*, strain CCGT11 was constructed. The cell growth was severely inhibited because the cells were unable to transport extracellular L-Phe to the intracellular compartment after knocking out *aroP*. The resulting cells were rendered unable to grow due to the lack of L-Phe. To further explore the effect of knocking out the *aroP* gene on growth, we proceeded to knock out *aroP* in CCGT10. When *tyrP* and *aroP* were knocked out simultaneously (strain CCGT12), CCGT12 also failed to grow normally due to the absence of L-Phe.

### Optimization of added amount of glucose

The adequacy of carbon supply is a key factor in determining titer to produce target chemicals using microorganisms [40]. In the experiments described above, a consistent glucose concentration of 40 g/L was used across all shake-flask incubations. To assess the effect of glucose concentration on L-Tyr production of CCGT10, with glucose as a carbon source, we tested six different concentrations: 20, 40, 60, 80, 100, and 120 g/L. Figure 3A reveals that cell growth was significantly inhibited at a glucose concentration of 20 g/L. However, as the glucose concentration exceeded 40 g/L, cell growth rates became similar. This suggested that an ample supply of carbon sources was advantageous for cellular proliferation. As shown in Fig. 3B, L-Tyr production was limited to 2.9 g/L at a glucose concentration of 20 g/L. When glucose concentration was low, strain CCGT10 produced lower levels of L-Tyr due to an insufficient supply of carbon sources during fermentation. Conversely, when the glucose concentration exceeded a certain threshold, it induced a change in the osmotic pressure of the

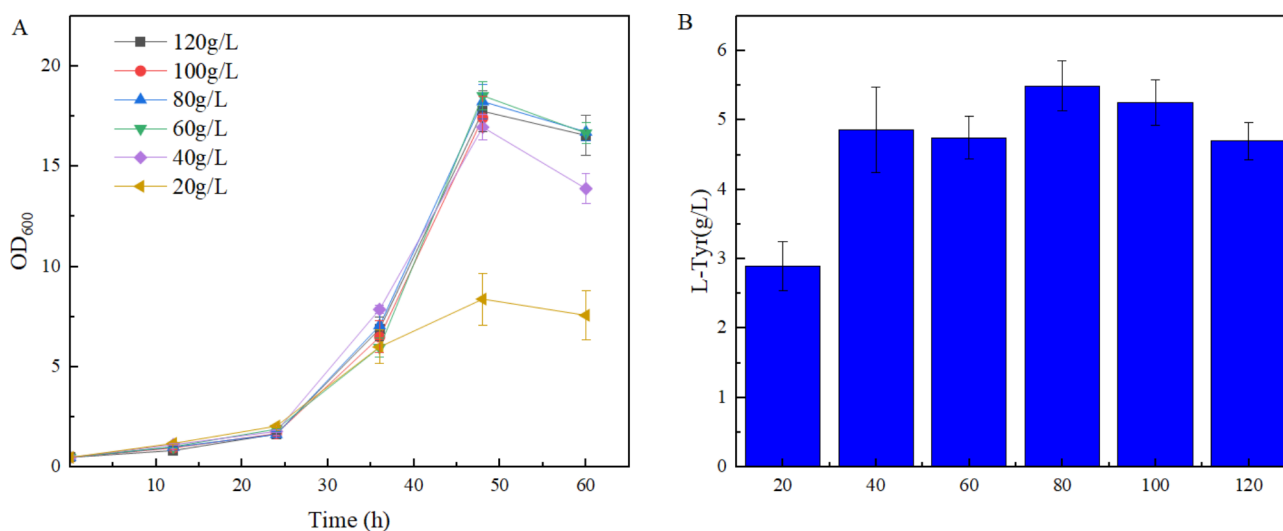


**Fig. 3** Optimization of the amount of glucose addition. **(A)** Cell growth curves of CCGT10 in different concentrations of glucose. **(B)** L-Tyr production of CCGT10 in different concentrations of glucose

fermentation broth, which negatively impacted the titer. The optimal L-Tyr production of 5.49 g/L was reached at a glucose concentration of 80 g/L. The consumption of glucose by strain CCGT10 at various glucose concentrations in the medium is presented in the Supplementary Material Fig. S2.

### Production of L-Tyr from mannitol

As the global population continues to swell, food issues are becoming increasingly prominent. Mannitol, recognized as a third-generation carbon source, has attracted researchers' attention because it does not compete with humans for carbon sources. Previous studies have demonstrated that the metabolic conversion of mannitol by microorganism results in an increased carbon flux to the EMP pathway and enhances the synthesis of the PEP, thereby promoting the biosynthesis of L-Tyr. The wild-type *C. crenatum* cannot utilize mannitol due to the presence of a mannitol inhibitory factor, MtlR, encoded by *mtlR*. Accordingly, we constructed CCMT01 by knocking out the *mtlR* gene from CCGT10. To investigate whether CCMT01 can effectively utilize mannitol as a carbon source, we added 40 g/L mannitol to CGXII medium as the sole carbon source and then tested the growth of CCTG10 and CCMT01. As shown in Fig. 4A, CCMT01 was able to grow normally, producing 1.39 g/L of L-Tyr within 60 h (Fig. 4B), whereas CCGT10 was unable to grow due to its inability to utilize mannitol.

In *C. crenatum*, *mtlTD* genes play crucial roles in mannitol absorption and utilization. The *mtlT* gene encodes the mannitol transporter, and the *mtlD* gene encodes the mannitol dehydrogenase [41]. To investigate the impact of *mtlD* on the absorption and utilization of mannitol, as well as the production of L-Tyr by CCMT01,  $P_{ncg10824}$  was used to overexpress *mtlD* (CCMT02) and co-overexpress *mtlTD* (CCMT03), respectively. The results depicted in Fig. 4A indicated that CCMT02, which solely overexpressed *mtlD*, outperformed CCMT03 in terms of growth and mannitol utilization. As shown in Fig. 4B, despite CCMT03 achieving a titer of 1.45 g/L, CCMT02 exhibited a higher L-Tyr titer of 1.56 g/L, marking an increase of 13.04% compared with CCMT01. Fructose-L-phosphate kinase, encoded by the *pfkB* gene, facilitates the conversion of fructose-L-phosphate into fructose-1,6-diphosphate, a key step in the transformation of mannitol into downstream products [42]. To delve deeper into the effects of different promoter strengths on cell growth and mannitol utilization, three distinct promoters were utilized to overexpress *pfkB* based on CCMT02. The strain using  $P_{ncg10824}$  was designated CCMT04, the one using  $P_{sod}$  as CCMT05, and the one using  $P_{eftu}$  as CCMT06. The data, presented in Fig. 4C, indicated that CCMT04 surpassed CCMT02 in growth and mannitol utilization. Surprisingly, as depicted in Fig. 4D,

the L-Tyr titer of CCMT04 reached 1.84 g/L, whereas those of CCMT05 and CCMT06 were lower than that of CCMT02, amounting 1.35 and 1.48 g/L, respectively.

To boost L-Tyr production through the use of mannitol, we examined the effects of varying mannitol concentrations on CCMT04's growth and L-Tyr production by establishing six mannitol gradients, mirroring the glucose concentration setup. Figure 4E illustrates that the normal growth of CCMT04 was markedly inhibited at a mannitol concentration of 20 g/L. When the concentration of mannitol exceeded 40 g/L, no significant difference was found in the growth of CCMT04. However, once the mannitol concentration surpassed 40 g/L, no significant changes in CCMT04's growth were observed. When mannitol concentration was low, strain CCMT04 produced lower levels of L-Tyr due to an insufficient supply of carbon sources during fermentation. Notably, at a mannitol concentration of 80 g/L in the fermentation medium, L-Tyr production peaked at 2.12 g/L, as depicted in Fig. 4F. The consumption of mannitol by strain CCMT04 at various concentrations of mannitol in the medium is presented in the Supplementary Material Fig. S3. This study marks the inaugural application of mannitol in L-Tyr synthesis and provides a foundational reference for its potential use in synthesizing other compounds.

### Co-production of L-Tyr using glucose and mannitol

In previous studies, researchers have observed that the production of compounds using mixed carbon sources generally exceeds that of single sources. For example, Eldin modified *C. glutamicum* to produce L-Tyr from glucose and xylose. The L-Tyr titer was 3.2 g/L with glucose as the sole carbon source and was 1.7 g/L with xylose as the sole carbon source. However, when a combination of glucose and xylose was utilized for L-Tyr production, the titer increased to 3.6 g/L at a glucose-to-xylose ratio of 1:3 [43]. In prior studies, strain CCMT04 produced L-Tyr using mannitol and glucose as carbon sources. Following concentration optimization, the optimal concentration of both carbon sources was determined to be 80 g/L when either glucose or mannitol was used individually for L-Tyr production. Consequently, we maintained a total carbon source concentration by combining 80 g/L of glucose with mannitol and explored the optimal conditions for L-Tyr production by varying the ratios of glucose to mannitol. The ratio of glucose to mannitol was set as 4:1, 3:1, 2:1, 1:1, 1:2, 1:3, and 1:4, respectively. As shown in Fig. 5A, the growth of CCMT04 was optimal when glucose constituted a larger proportion of the mixed carbon source. When the ratio of glucose-to-mannitol fell below 3:1, L-Tyr production decreased with increased proportion of mannitol. At a glucose-to-mannitol ratio of 3:1, L-Tyr production peaked among the seven groups, reaching 6.42 g/L. The curves comparing glucose and mannitol

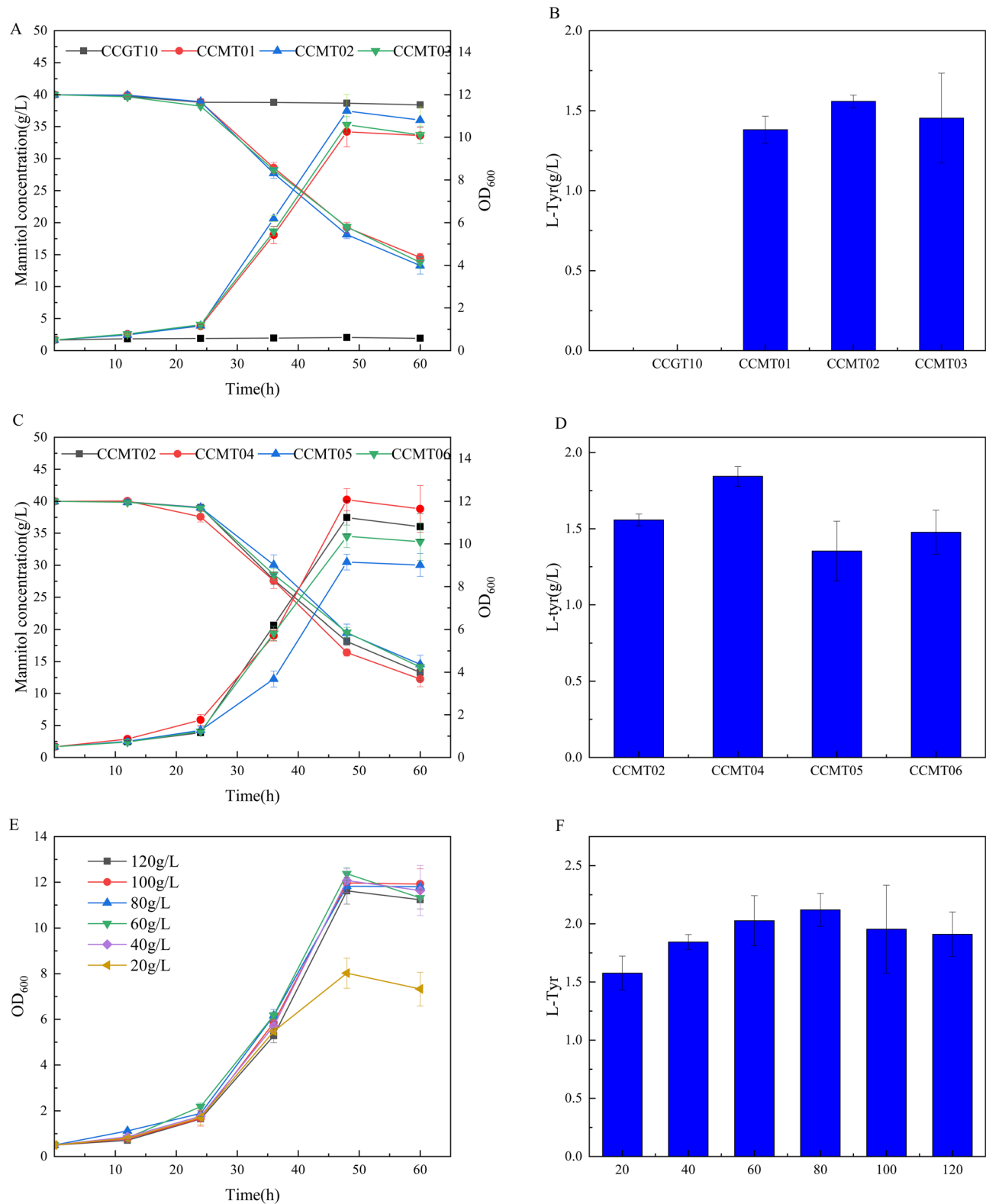


**Fig. 4** Shake-flask fermentation parameters using mannitol as a carbon source. **(A)** Cell growth and mannitol-consumption curves of strains with *mtlR* knockout and *mtlTD* genes overexpression. **(B)** L-Tyr production in strains with *mtlR* gene knocked out and *mtlTD* genes overexpressed. **(C)** Cell growth and mannitol-consumption curves of strains by using three different strength promoters to overexpress the *pfkB* gene. **(D)** L-Tyr production by using three different strength promoters to overexpress the *pfkB* gene. **(E)** Cell growth and mannitol-consumption curves of CCMT04 in different concentrations of mannitol. **(F)** L-Tyr production of CCMT04 in different concentrations of mannitol

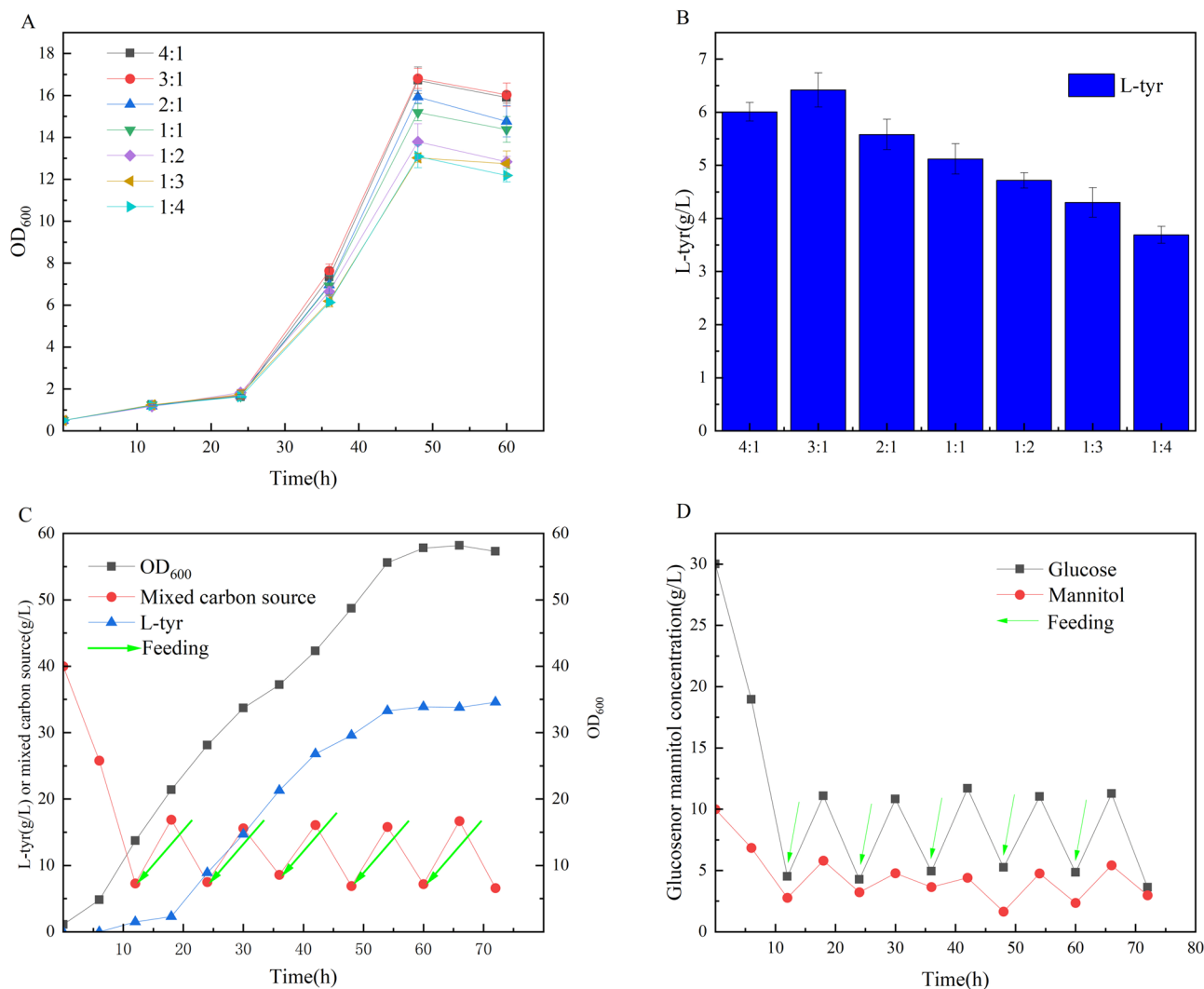


**Fig. 5** Fermentation parameters using mixed carbon sources of CCMT04. **(A)** Cell-growth curves of CCMT04 in different ratios of glucose and mannitol. **(B)** L-Tyr production of CCMT04 in different ratios of glucose and mannitol. **(C)** Cell growth, L-Tyr production and total carbon source curves of CCMT04 in a 5 L bioreactor. **(D)** Glucose and mannitol-consumption curves of CCMT04 in a 5 L bioreactor

at various ratios can be found in the Supplementary Material Fig. S4. At this juncture, the shake-flask fermentation titer surpassed the maximum L-Tyr titer of *C. glutamicum*.

To enhance the L-Tyr titer of *C. crenatum* CCMT04 strain, we investigated the fermentation of the CCMT04 strain through fed-batch fermentation by using a 5 L bioreactor. Throughout the fermentation process, we used 1 mol/L HCL solution or ammonia to adjust the pH and ensure that the fermentation pH was stabilized at 7–7.5. When the concentration of the mixed carbon source in the fermenter dropped to 10 g/L, nutrients of pre-inactivated bacteria containing 600 g/L mixed carbon source (450 g/L glucose and 150 g/L mannitol), 40 g/L (NH<sub>4</sub>)<sub>2</sub>SO<sub>4</sub>, and 10 g/L yeast extract were supplemented therein. The fermentation broth was sampled every 6 h to monitor the OD<sub>600</sub>, mixed carbon content, and L-Tyr

production during fermentation. After 72 h of fermentation, the highest OD<sub>600</sub> of the strain reached 58.2, and the highest L-Tyr production reached 34.6 g/L. The variations in glucose and mannitol during the fermentation process are illustrated in Fig. 5D. The titer of the fed-batch fermentation also exceeded the maximum titer of *C. glutamicum*.

### Discussion

This was the first time that mannitol was utilized in the synthesis of L-Tyr. In past studies, researchers have primarily focused on modifying strains to produce L-Tyr from glucose. For example, Cheol et al. optimized the expression of the *ppsA* gene by incorporating a short 5'-UTR before the *ppsA* gene to enhance the supply of PEP during the process, resulting in an L-Tyr titer of 3.0 g/L [44].

In recent years, researchers have increasingly focused on alternative sources of carbon. Acetate is a very abundant and inexpensive carbon source that is often generated as a by-product during the pretreatment of lignocellulosic biomass [45]. Jo et al. demonstrated the modulation of carbon-flux distribution between glyoxylate and TCA cycles in *E. coli*. The production of tyrosine by *E. coli* using acetate was achieved, and the titer reached 0.7 g/L [46]. Xylose is second only to glucose in carbon source [47]. Significant potential holds for the production of chemicals from xylose. By using parallel metabolic engineering to separate the glucose and xylose utilization pathways in *E. coli*, Fujiwara et al. significantly enhanced the efficiency of xylose utilization. This enhancement led to a final L-Tyr titer of 1.34 g/L, which was 173% higher than that of the control group [48].

Mannitol, a simple six-membered alcohol, can be typically synthesized from marine macroalgae, which are characterized by rapid growth and widespread distribution [49]. Therefore, mannitol neither compete with human food sources nor required as complex production processes as glucose.

When mannitol is used as a fermentation carbon source, the carbon flux is predominantly directed toward the EMP, resulting in increased production of PEP, an important precursor in the L-Tyr. However, the wild-type *C. glutamicum* strain, due to the presence of the mannitol inhibitory factor MtlR encoded by *mtlR* gene, cannot utilize mannitol. To enable *C. glutamicum* to utilize mannitol, Hoffmann et al. engineered the organism to grow in a medium with mannitol as the sole carbon source by deleting the *mtlR* gene [50].

In the present study, we engineered a strain of *C. crenatum*, enabling it to produce L-Tyr from glucose by the inhibition of competing metabolic pathways, enhancement of precursor synthesis, and modification of transporter proteins. Subsequently, the overexpression of *mtlD* and *pfkB*, achieved through knockout of *mtlR*, allowed the strain to utilize mannitol as the sole carbon source for L-Tyr production. Subsequently, by adjusting the ratio of glucose to mannitol as carbon source, we achieved a titer of 6.42 g/L and a fed-batch fermentation titer of 34.6 g/L, both surpassing the maximum L-Tyr titer previously reported for *C. glutamicum*.

However, this approach is not optimal for culture with mixed carbon sources. When glucose is utilized with other carbon sources, cells tend to prefer glucose due to its simplicity. This preference significantly hinders their utilization of other carbon sources in the presence of glucose [51]. Numerous efforts have been exerted by researchers to alleviate carbon catabolite repression. For example, Zhou alleviated carbon catabolite repression to some extent by knocking out the cyclic adenosine monophosphate synthesis pathway, resulting in a 43.1%

increase in the titer of patchesoulol [52]. Gao replaced the original promoters with strong promoters to eliminate sensitivity to glucose effects in the key enzymes of the xylose metabolism pathway, leading to a 193% increase in xylose utilization [53].

In the next phase of our research, we will focus on how to make the co-utilization of glucose and mannitol more coordinated. Additionally, we will continue our efforts to broaden the range of applications for chemicals produced from mannitol.

## Conclusions

L-Tyr, a crucial aromatic amino acid, is extensively utilized in various industries including food, pharmaceuticals, cosmetics, and beyond. In this study, we utilized genetic engineering methods to modify *C. crenatum*, allowing it to harness glucose and mannitol for L-Tyr production. Our results revealed that when solely utilizing glucose as the carbon source, an L-Tyr titer of 5.49 g/L was achieved. Mannitol, on its own, generated an L-Tyr titer of 2.12 g/L. Notably, the combination of glucose and mannitol in a 3:1 ratio as a mixed carbon source elevated the L-Tyr titer to 6.42 g/L. Moreover, through fed-batch fermentation, the titer soared to 34.6 g/L. These titers surpass the maximum productivity observed in *C. glutamicum*.

## Supplementary Information

The online version contains supplementary material available at <https://doi.org/10.1186/s12934-024-02564-1>.

Supplementary Material 1

## Acknowledgements

This work was supported by the School of Life Sciences and the School of Health at Jiangxi Normal University.

## Author contributions

G: investigation, the main data curation, writing - original draft; S: writing - review & editing, data curation; M: instruction, methodology; B: data curation, methodology; Y: investigation, methodology; X: conceptualization, writing - review & editing, instruction, supervision. All authors reviewed the manuscript.

## Funding

This work was supported by National Natural Science Foundation of China (32260014) and Key Project of Jiangxi Provincial Natural Science Foundation(20202ACBL205001).

## Data availability

No datasets were generated or analysed during the current study.

## Declarations

## Competing interests

The authors declare no competing interests.

Received: 5 August 2024 / Accepted: 10 October 2024

Published online: 22 October 2024

## References

- Kumar Patel M, Fanyuk M, Feynberg O, et al. Phenylalanine induces mango fruit resistance against chilling injuries during storage at suboptimal temperature. *Food Chem.* 2023;134909. <https://doi.org/10.1016/j.foodchem.2022.134909>. 405 (Pt B):.
- Tachikawa Y, Okuno M, Itoh T, Hirasawa T. Metabolic engineering with adaptive laboratory evolution for phenylalanine production by *Corynebacterium glutamicum*. *J Biosci Bioeng.* 2024;137(5):344–53. <https://doi.org/10.1016/j.jbiosc.2024.01.006>.
- Li S, Cai Y, Guan T, et al. Quinic acid alleviates high-fat diet-induced neuroinflammation by inhibiting DR3/IKK/NF- $\kappa$ B signaling via gut microbial tryptophan metabolites. *Gut Microbes.* 2024;16(1):2374608. <https://doi.org/10.1080/19490976.2024.2374608>.
- Zucca FA, Capucciati A, Bellei C, et al. Neuromelanins in brain aging and Parkinson's disease: synthesis, structure, neuroinflammatory, and neurodegenerative role. *IUBMB Life.* 2023;75(1):55–65. <https://doi.org/10.1002/iub.2654>.
- Zhu TT, Wang H, Gu HW, et al. Melanin-like polydopamine nanoparticles mediating anti-inflammatory and rescuing synaptic loss for inflammatory depression therapy. *J Nanobiotechnol.* 2023;21(1):52. <https://doi.org/10.1186/s12951-023-01807-4>. Published 2023 Feb 10.
- Lin W, Wang X, Diao M, et al. Promoting reactive oxygen species accumulation to overcome tyrosine kinase inhibitor resistance in cancer. *Cancer Cell Int.* 2024;24(1):239. <https://doi.org/10.1186/s12935-024-03418-x>. Published 2024 Jul 9.
- Ibrahim GG, Perera M, Abdulmalek SA, Yan J, Yan Y. De Novo Synthesis of Resveratrol from sucrose by metabolically Engineered *Yarrowia Lipolytica*. *Bio-molecules.* 2024;14(6):712. <https://doi.org/10.3390/biom14060712>. Published 2024 Jun 16.
- Yuan SF, Yi X, Johnston TG, Alper HS. De novo resveratrol production through modular engineering of an *Escherichia coli*-*Saccharomyces cerevisiae* co-culture. *Microb Cell Fact.* 2020;19(1):143. <https://doi.org/10.1186/s12934-020-01401-5>. Published 2020 Jul 14.
- Xu S, Zhang Y, Li Y, Xia X, Zhou J, Shi G. Production of L-tyrosine using tyrosine phenol-lyase by whole cell biotransformation approach. *Enzyme Microb Technol.* 2019;131:109430. <https://doi.org/10.1016/j.enzmictec.2019.109430>.
- Mujumdar P, Kopecka J, Bua S, Supuran CT, Riganti C, Poulsen SA. Carbonic anhydrase XII inhibitors overcome Temozolomide Resistance in Glioblastoma. *J Med Chem.* 2019;62(8):4174–92. <https://doi.org/10.1021/acs.jmedchem.9b00282>.
- Lütke-Eversloh T, Santos CN, Stephanopoulos G. Perspectives of biotechnological production of L-tyrosine and its applications. *Appl Microbiol Biotechnol.* 2007;77(4):751–62. <https://doi.org/10.1007/s00253-007-1243-y>.
- McCarty NS, Ledesma-Amaro R. Synthetic Biology tools to engineer microbial communities for Biotechnology. *Trends Biotechnol.* 2019;37(2):181–97. <https://doi.org/10.1016/j.tibtech.2018.11.002>.
- Zou G, Nielsen JB, Wei Y. Harnessing synthetic biology for mushroom farming. *Trends Biotechnol.* 2023;41(4):480–3. <https://doi.org/10.1016/j.tibtech.2022.10.001>.
- Kim B, Binkley R, Kim HU, Lee SY. Metabolic engineering of *Escherichia coli* for the enhanced production of L-tyrosine. *Biotechnol Bioeng.* 2018;115(10):2554–64. <https://doi.org/10.1002/bit.26797>.
- Ikeda M, Okamoto K, Katsumata R. Cloning of the transketolase gene and the effect of its dosage on aromatic amino acid production in *Corynebacterium glutamicum*. *Appl Microbiol Biotechnol.* 1999;51(2):201–6. <https://doi.org/10.1007/s002530051382>.
- Guo X, Wu X, Ma H, Liu H, Luo Y. Yeast. A platform for the production of L-tyrosine derivatives. *Yeast.* 2023;40(5–6):214–30. <https://doi.org/10.1002/yea.3850>.
- Ikeda M, Katsumata R. Metabolic Engineering to produce tyrosine or phenylalanine in a tryptophan-producing *Corynebacterium glutamicum* strain. *Appl Environ Microbiol.* 1992;58(3):781–5. <https://doi.org/10.1128/aem.58.3.781-785.1992>.
- Huang M, Liu W, Qin C, Xu Y, Zhou X, Wen Q, Ma W, Huang Y, Chen X. Copper resistance mechanism and copper response genes in *Corynebacterium Crenatum*. *Microorganisms.* 2024;12(5):951. <https://doi.org/10.3390/microorganisms12050951>.
- Yang F, Xu J, Zhu Y, Wang Y, Xu M, Rao Z. High-level production of the agmatine in engineered *Corynebacterium crenatum* with the inhibition-releasing arginine decarboxylase. *Microb Cell Fact.* 2022;21(1):16. <https://doi.org/10.1186/s12934-022-01742-3>.
- Huang M, Zhu L, Feng L, Zhan L, Zhao Y, Chen X. Reforming nitrate metabolism for enhancing L-Arginine production in *Corynebacterium Crenatum* under Oxygen Limitation. *Front Microbiol.* 2022;13:834311. <https://doi.org/10.3389/fmicb.2022.834311>.
- Zhang X, Han R, Bao T, Zhao X, Li X, Zhu M, Yang T, Xu M, Shao M, Zhao Y, Rao Z. Synthetic engineering of *Corynebacterium crenatum* to selectively produce acetoin or 2,3-butanediol by one step bioconversion method. *Microb Cell Fact.* 2019;18(1):128. <https://doi.org/10.1186/s12934-019-1183-0>.
- Chen X, Wu X, Jiang S, Li X. Influence of pH and neutralizing agent on anaerobic succinic acid production by a *Corynebacterium crenatum* strain. *J Biosci Bioeng.* 2017;124(4):439–44. <https://doi.org/10.1016/j.jbiosc.2017.04.021>.
- Xiao W, He M. Characteristics, regional differences, and influencing factors of China's water-energy-food (W-E-F) pressure: evidence from Dagum Gini coefficient decomposition and PGTWR model. *Environ Sci Pollut Res Int.* 2023;30(24):66062–79. <https://doi.org/10.1007/s11356-023-27010-4>.
- Pérez-García F, Klein VJ, Brito LF, Brautaset T. From Brown Seaweed to a sustainable Microbial Feedstock for the production of Riboflavin. *Front Bioeng Biotechnol.* 2022;10:863690. <https://doi.org/10.3389/fbioe.2022.863690>. Published 2022 Apr 12.
- Sheng Q, Wu X, Jiang Y, Li Z, Wang F, Zhang B. Highly efficient biosynthesis of L-ornithine from mannitol by using recombinant *Corynebacterium glutamicum*. *Bioresour Technol.* 2021;327:124799. <https://doi.org/10.1016/j.biortech.2021.124799>.
- Zhu C, You X, Wu T, Li W, Chen H, Cha Y, Zhuo M. Efficient utilization of carbon to produce aromatic valencene in *Saccharomyces cerevisiae* using mannitol as the substrate. *Green Chem.* 2022;24:4614. <https://doi.org/10.1111/j.1567-1364.2003.tb00134.x>.
- Hoffmann SL, Jungmann L, Schiefelbein S, et al. Lysine production from the sugar alcohol mannitol: design of the cell factory *Corynebacterium glutamicum* SEA-3 through integrated analysis and engineering of metabolic pathway fluxes. *Metab Eng.* 2018;47:475–87. <https://doi.org/10.1016/j.ymben.2018.04.019>.
- Xu J, Zhang J, Han M, Zhang W. A method for simultaneous gene overexpression and inactivation in the *Corynebacterium glutamicum* genome. *J Ind Microbiol Biotechnol.* 2016;43(10):1417–27. <https://doi.org/10.1007/s10295-016-1806-y>.
- Xu JZ, Zhang WG. Strategies used for genetically modifying bacterial genome: site-directed mutagenesis, gene inactivation, and gene overexpression. *J Zhejiang Univ Sci B.* 2016;17(2):83–99. <https://doi.org/10.1631/jzus.1500187>.
- Jäger W, Schäfer A, Pühler A, Labes G, Wohlleben W. Expression of the *Bacillus subtilis* *sacB* gene leads to sucrose sensitivity in the gram-positive bacterium *Corynebacterium glutamicum* but not in Streptomyces lividans. *J Bacteriol.* 1992;174(16):5462–5. <https://doi.org/10.1128/jb.174.16.5462-5465.1992>.
- Mutz M, Brüning V, Brüsseler C, Müller MF, Noack S, Marienhagen J. Metabolic engineering of *Corynebacterium glutamicum* for the production of anthranilate from glucose and xylose. *Microb Biotechnol.* 2024;17(1):e14388. <https://doi.org/10.1111/1751-7915.14388>.
- Surwase SN, Patil SA, Apine OA, Jadhav JP. Efficient microbial conversion of L-tyrosine to L-DOPA by *Brevundimonas sp. SGJ*. *Appl Biochem Biotechnol.* 2012;167(5):1015–28. <https://doi.org/10.1007/s12010-012-9564-4>.
- Nie L, He Y, Hu L, Zhu X, Wu X, Zhang B. Improvement in L-ornithine production from mannitol via transcriptome-guided genetic engineering in *Corynebacterium glutamicum*. *Biotechnol Biofuels Bioprod.* 2022;15(1):97. <https://doi.org/10.1186/s13068-022-02198-8>. Published 2022 Sep 19.
- Zhang P, Gao J, Zhang H, et al. Metabolic engineering of *Escherichia coli* for the production of an antifouling agent zosteric acid. *Metab Eng.* 2023;76:247–59. <https://doi.org/10.1016/j.ymben.2023.02.007>.
- Zhou S, Hao T, Zhou J. Fermentation and Metabolic Pathway Optimization to De Novo Synthesize (2S)-Naringenin in *Escherichia coli*. *J Microbiol Biotechnol.* 2020;30(10):1574–82. <https://doi.org/10.4014/jmb.2008.08005>.
- Gosset G, Yong-Xiao J, Berry A. A direct comparison of approaches for increasing carbon flow to aromatic biosynthesis in *Escherichia coli*. *J Ind Microbiol.* 1996;17(1):47–52. <https://doi.org/10.1007/BF01570148>.
- Patnaik R, Liao JC. Engineering of *Escherichia coli* central metabolism for aromatic metabolite production with near theoretical yield. *Appl Environ Microbiol.* 1994;60(11):3903–8. <https://doi.org/10.1128/aem.60.11.3903-3908.1994>.
- Gao S, Ma D, Wang Y, Zhang A, Wang X, Chen K. Whole-cell catalyze L-dopa to dopamine via co-expression of transport protein AroP in *Escherichia coli*. *BMC Biotechnol.* 2023;23(1):33. <https://doi.org/10.1186/s12896-023-00794-6>. Published 2023 Aug 29.
- Wu J, Liu Y, Zhao S, Sun J, Jin Z, Zhang D. Application of dynamic regulation to increase L-Phenylalanine production in *Escherichia coli*. *J Microbiol Biotechnol.* 2019;29(6):923–32. <https://doi.org/10.4014/jmb.1901.01058>.

40. Zou XZ, Gong LC, Li TT, Lv SY, Wang J. Optimization of fermentation conditions for the production of  $\gamma$ -aminobutyric acid by *Lactobacillus hilgardii* GZ2 from traditional Chinese fermented beverage system. *Bioprocess Biosyst Eng*. 2024;47(6):957–69. <https://doi.org/10.1007/s00449-024-03028-x>.
41. Peng X, Okai N, Vertès AA, Inatomi K, Inui M, Yukawa H. Characterization of the mannitol catabolic operon of *Corynebacterium glutamicum*. *Appl Microbiol Biotechnol*. 2011;91(5):1375–87. <https://doi.org/10.1007/s00253-011-3352-x>.
42. Wang Z, Chan SHJ, Sudarsan S, Blank LM, Jensen PR, Solem C. Elucidation of the regulatory role of the fructose operon reveals a novel target for enhancing the NADPH supply in *Corynebacterium glutamicum*. *Metab Eng*. 2016;38:344–57. <https://doi.org/10.1016/j.ymben.2016.08.004>.
43. Kurpejović E, Burgardt A, Bastem GM, Junker N, Wendisch VF, Sariyar Akbulut B. Metabolic engineering of *Corynebacterium glutamicum* for l-tyrosine production from glucose and xylose. *J Biotechnol*. 2023;363:8–16. <https://doi.org/10.1016/j.jbiotec.2022.12.005>.
44. Kim SC, Min BE, Hwang HG, Seo SW, Jung GY. Pathway optimization by re-design of untranslated regions for L-tyrosine production in *Escherichia coli*. *Sci Rep*. 2015;5:13853. <https://doi.org/10.1038/srep13853>. Published 2015 Sep 8.
45. Wierckx N, Koopman F, Bandounas L, de Winde JH, Ruijsenaars HJ. Isolation and characterization of *Cupriavidus basilensis* HMF14 for biological removal of inhibitors from lignocellulosic hydrolysate. *Microb Biotechnol*. 2010;3(3):336–43. <https://doi.org/10.1111/j.1751-7915.2009.00158.x>.
46. Jo M, Noh MH, Lim HG, et al. Precise tuning of the glyoxylate cycle in *Escherichia coli* for efficient tyrosine production from acetate. *Microb Cell Fact*. 2019;18(1):57. <https://doi.org/10.1186/s12934-019-1106-0>. Published 2019 Mar 19.
47. Elmore JR, Dexter GN, Salvachúa D et al. Engineered *Pseudomonas putida* simultaneously catabolizes five major components of corn stover lignocellulose: Glucose, xylose, arabinose, p-coumaric acid, and acetic acid. *Metab Eng*. 2020;62:62–71. *Metabolic engineering*, 62, 62–71. <https://doi.org/10.1016/j.ymben.2020.08.001>
48. Fujiwara R, Noda S, Tanaka T, Kondo A. Metabolic engineering of *Escherichia coli* for shikimate pathway derivative production from glucose-xylose co-substrate. *Nat Commun*. 2020;11(1):279. <https://doi.org/10.1038/s41467-019-14024-1>. Published 2020 Jan 14.
49. Zozaya-Valdés E, Roth-Schulze AJ, Thomas T. Effects of temperature stress and Aquarium conditions on the Red Macroalga *Delisea pulchra* and its Associated Microbial Community. *Front Microbiol*. 2016;7. <https://doi.org/10.3389/fmicb.2016.00161>. 161. Published 2016 Feb 18.
50. Hoffmann SL, Kohlstedt M, Jungmann L, et al. Cascaded valorization of brown seaweed to produce l-lysine and value-added products using *Corynebacterium glutamicum* streamlined by systems metabolic engineering. *Metab Eng*. 2021;67:293–307. <https://doi.org/10.1016/j.ymben.2021.07.010>.
51. Zhao C, Sinumvayo JP, Zhang Y, Li Y. Design and development of a Y-shaped microbial consortium capable of simultaneously utilizing biomass sugars for efficient production of butanol. *Metab Eng*. 2019;55:111–9. <https://doi.org/10.1016/j.ymben.2019.06.012>.
52. Zhou L, Wang Q, Shen J, et al. Metabolic engineering of glycolysis in *Escherichia coli* for efficient production of patchoulol and  $\tau$ -cadinol. *Bioresour Technol*. 2024;130004. <https://doi.org/10.1016/j.biortech.2023.130004>. 391(Pt B):.
53. Gao M, Zhao Y, Yao Z, Su Q, Van Beek P, Shao Z. Xylose and shikimate transporters facilitates microbial consortium as a chassis for benzyloisoquinoline alkaloid production. *Nat Commun*. 2023;14(1):7797. <https://doi.org/10.1038/s41467-023-43049-w>. Published 2023 Nov 28.

### Publisher's note

Springer Nature remains neutral with regard to jurisdictional claims in published maps and institutional affiliations.